SV-Training and Kernel Change Detection Algorithm for the Abrupt Modification in EMI Data for Buried Metallic Target Localization and Identification

Yacine Matriche [1,2,3,*], Saïd Moussaoui [4], Mouloud Feliachi [3], Abdelhalim Zaoui [2], and Mehdi Abdellah [2]

[1] EST, Kolea Tipaza, Algeria

[2] Ecole Militaire Polytechnique, BP 17, B. E. Bahri, Algiers, Algeria

[3] Université de Nantes, PRES-L'UNAM, IREENA, CRTT, Bd de l'Université, BP 406, St-Nazaire Cedex 44602, France.

[4] Ecole Centrale de Nantes, IRCCYN, UMR CNRS 6597, 1 rue de la Noë, 44321 Nantes, France
*yacine.matriche@etu.univ-nantes.fr

Abstract ─ In this paper, we propose a new method to identify and to locate buried metallic object in ElectroMagnetic Induction (EMI) data based on the Kernel Change Detection (KCD) algorithm. The signature of the object in the EMI data is typically of low amplitude. Particularly, in the case where two objects are located at different depths, the amplitude of the deeper buried object is negligible compared to that of the object buried in the first centimeter of the soil. This would result in the fact that, the EMI system can neglect the signature of this object and consequently increases miss rate or False Negative Rate (FNR). The aim of the proposed method is to calculate a decision index for each EMI measurement in a so-called hypotheses space using KCD algorithm. The amplitude of these decision indexes in the case of objects at different depths are in the same range, which make their variance smaller. Indeed, this index will be compared to a threshold for judging the presence or absence of a rupture. The validation of the proposed method is performed by processing real EMI data derived from a series of measurements on real objects.

Index Terms ─ Decision index, electromagnetic induction, kernel change detection algorithm, mine detection, support vector training.

I. INTRODUCTION

Many countries around the world are affected by mines and UneXploded Ordnance (UXO). These remains threaten of the human being because their impacts still exist and can occur at any time. To fight against these threats, the researchers have developed several detection systems such as ElectroMagnetic Induction (EMI) system [1], [2] and the Ground-Penetrating Radar (GPR) [3].

The EMI system is the first prospecting system that was developed for the exploration of near basement. It is used in the geophysical survey to locate the metallic structures and objects inside the upper layer of the soil. It has been used in the field of demining during the First World War. Since then, the researchers developed it by increasing its sensitivity to find smaller amounts of metal. The first EMI system contains only a single coil [4]. Subsequently, researchers have added other coils in order to distinguish between a dummy object and a mine. The most recent EMI operates with low range frequencies (typically 1 kHz to 1 MHz) and its operating principle is quite simple. The interaction between the magnetic field and the metallic structures gives rise to eddy currents that generate a secondary field which will oppose the primary field. The use of EMI systems has become more interesting with the development of data processing

Submitted On: April 30, 2014
Accepted On: October 5, 2014

techniques based on inverse methods [1], [4].

In this context, we can mention the paper [5] in which a Normalized Surface Magnetic Source (NSMS) model is applied to UXO discrimination. A fast and accurate numerical forward model that represents an objects response using a set of equivalent magnetic dipoles distributed on a surrounding closed surface. In [6], the authors present a methodology to guarantee the convergence of the electromagnetic inverse method. It consists of using Genetic Algorithms (GA) to identify a model that will be used to estimate the electric and magnetic field radiated by the device under test. In [7], the authors propose a novel scheme for detecting the location of a metallic mine. This technique takes into account Eddy-Current Response (ECR) induced on the conducting marine mines as well as Current-Channeling Response (CCR) associated with the perturbation of currents induced in the conductive marine environment.

In [1], an Improved Particle Swarm Optimization (IPSO) and Finite Element Method (FEM) are used to inverse the EMI data. This method leads to interesting results in terms of identification and localization of buried object. However, and despite of its effectiveness, the application of the FEM method makes the exploration in the real-time almost impossible, resulting in the necessity to resort to high performance computing devices. In order to have a pre-decision in real-time about the existence of a suspicious object, we must use a faster inversion method.

In this paper, we propose a fast processing method for the EMI data based on the Kernel Change Detection (KCD) algorithm [8], [9]. It consists of detecting the ruptures due to Abrupt Change (AC) in the EMI observations (EMI measurements). The AC detection is not directly detected in the observations space, but rather in a hypotheses space using a Kernel and Support Vector (SV) training in order to obtain a data representation in this space [10], [8], [9]. Consequently, a decision index is calculated for each position of the EMI system [11]. After that, we build an image from the resulting decision index where the shape of objects is apparent.

However, even if the resulting image is not well filtered because of the roughness of the soil, the decision index of the object shall prevail and an adequate threshold will give us a clear shape of the object. Finally, the inference on the presence or the absence of the object will thus be performed with a reduced rate of false alarms.

The rest of this paper is organized as follows. In Section II, the EMI system will be presented and its basic operation will be explained. Then, in Section III, the KCD algorithm will be presented in detail, the rupture detection method using the SV estimators will be also presented in this section. Finally, in Section IV, we will adapt the KCD method to the EMI data and will detail the followed steps. The adjusting of the KCD parameters to the EMI data is also presented in this section. The effectiveness of the proposed method is tested on a real EMI data.

II. ELECTROMAGNETIC INDUCTION SYSTEM

The basic EMI system consists of a transmitter coil and two receiver coils, Fig. 1. Its operation is based on electromagnetic induction, where the transmitter coil, traversed by a variable current, generates an electromotive force across the two receiver coils disposed above and below it at the same distance [1]. In vacuum, the difference of the induced voltage (ΔV) between the two receiving coils is zero. During prospection and when the system passes over a metallic object, the transmitter coil generates an eddy current in the surface of this object. Therefore, these currents will generate an electromotive force which is only across the lower receiver coil and the balance between the two induced voltages in the receiver coils is disturbed. Thus, the ΔV quantity depends only on the field generated by the eddy current on the buried object. In this case, the ΔV gives the signature of the object since the generated field depends on its physical and geometrical characteristics [1], [4].

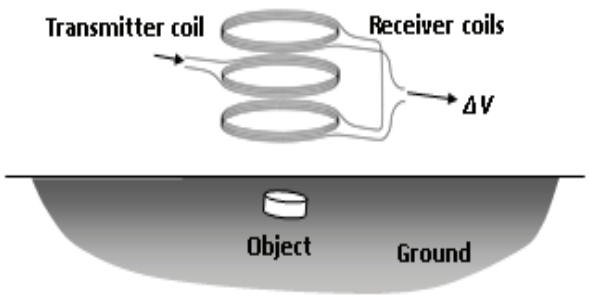

Fig. 1. Basic diagram of EMI system.

III. KERNEL CHANGE DETECTION ALGORITHM

A. General framework

AC detection in signals is a much studied problem in the signal processing literature [10] [12]. In the case of systems where the data, defined in the observation space $\mathcal{X}$ follow a known physical or statistical model according to some Probability Density Function (PDF), this task has become a simple and easy to implement. However, when the PDF is unknown, one has to use unsupervised statistical methods based on machine learning [10], [13].

In that respect, the KCD algorithm, proposed in [8], [9], finds a minimal decision region $R_x^{\mathcal{X}} \in \mathcal{X}$ where most of the data $(x_i;\, i=1,\ldots,m)$ have the same unknown PDF. The region $R_x^{\mathcal{X}}$ is defined by a representation based on a real valued decision function $f(\cdot)$, according to:

$$f(x) \geq 0, x \in R_x^{\mathcal{X}} \text{ and } f(x) < 0, x \notin R_x^{\mathcal{X}}, \quad (1)$$

with a decision function $f(\cdot)$ deduced by training a single class SVM classifier [10], [12].

B. SVM training for AC detection

Let $\boldsymbol{x} = f(x_1; x_2, \ldots, x_m) \in \mathcal{X}$ a training vector. The aim of single-class classification is the estimation of a region $R_x^X \in X$ in which the decision functions $f(\cdot) \geq 0$. In this case, we defined another space $\mathcal{F}$, where the estimate of an image of the $R_x^{\mathcal{X}}$ is possible. Let ϕ a mapping function defined over the input space $\mathcal{X}$ and taking values in hypotheses space as follows:

$$\phi : \mathcal{X} \times \mathcal{X} \rightarrow \mathcal{F} \quad (2)$$
$$< x_i, x_j > \rightarrow < \phi_i, \phi_j >.$$

Here, $\mathcal{F}$ is endowed with a dot product $< \cdot, \cdot > = k(\cdot, \cdot)$, where $k(\cdot, \cdot)$ is a normalized kernel and it fulfills the Mercer conditions where $\{\forall (x_i, x_j) \in \mathcal{X}, k(x_i, x_j) > 0 \text{ and } k(x_i, x_i) = 1\}$. In this case, all the images of the inputs $(x_i \in \mathcal{X})$ in $\mathcal{F}$ lie-on the perimeter of a circle with a unit radius and center O (O is also the center of $\mathcal{F}$), as shown in Fig. 2 (a). Therefore, the single-class SVM for the AC detection estimation consists in separating the training vectors from the hypersphere center O with a hyperplane $\mathcal{W}$ such that $\{< w,\, x >_{\mathcal{F}} - b = 0$ with $w \in \mathcal{F}$ and $b \in \mathbb{R}_+^*\}$.

However, the term $< w,\, x_i >$ can be computed using only the dot product function $k(x_i,\, x_j) = < x_i,\, x_j >$ [11]. This kernel represents a dot product in some feature space if it fulfills the Mercer conditions [8]. These conditions are satisfied for a wide range of kernels, including Gaussian radial basis functions defined as [9]:

$$k(x_i, x_j) = exp\left(-\frac{\left\| x_i - x_j \right\|_{\mathcal{X}}^2}{2\sigma^2} \right), \quad (3)$$

where σ is a parameter that controls the dispersion of the images ϕ_i of the observations x_i.

The decision function $f(\cdot)$ in equation 1 will therefore be defined as:

$$f(x_i) = < w,\, x_i >_{\mathcal{F}} - b. \quad (4)$$

Consequently, this decision function, defined in the hypotheses space $\mathcal{F}$, will allow to deduce the region $R_x^{\mathcal{X}}$ in the input $\mathcal{X}$. Thus, SVM approach for the AC detection returns to the maximization of the distance between the center O of the hypersphere and the hyperplane $\mathcal{W}$ by solving the following optimization problem:

$$min\left(\frac{1}{2} \|w\|_{\mathcal{F}}^2 + \frac{1}{vm} \sum_{i=1}^{m} \xi_i - b \right), \quad (5)$$

where $w \in \mathcal{F}, b \in \mathbb{R}_+^*$ and $\xi_i \in \mathbb{R}^m$, subject to:

$$< w,\, x_i >_{\mathcal{F}} - b \geq \xi_i \text{ and } \xi_i \geq 0, \quad (6)$$

where $\frac{1}{vm}$ is a positive parameter that tunes the possible amount of outliers and ξ_i are the so-called slack variables, added here to take-outliers [9].

In Fig. 2 (a), there are some observations which are not in above of the hyperplane $\mathcal{W}$. To take into account these observations, a smooth margin ξ_i is added in equation (5) for each observation x_i.

The minimization problem defined in equation (5) is quadratic with linear constraints. Adding the Lagrange multipliers $\alpha_i, i = 1, \ldots, m,$ brings back to the following dual minimization problem:

$$\min_{\alpha} \frac{1}{2} \boldsymbol{\alpha}^t \, \boldsymbol{K} \, \boldsymbol{\alpha}, \quad (7)$$

subject to:

$$0 \le \alpha_i \le \frac{1}{vm} \text{ and } \sum_{i=1}^{m} \alpha_i = 1, \ (\forall i = 1,\ldots,m), \quad (8)$$

which can be solved by numerical methods of quadratic programming [14], [15], where $\boldsymbol{K}$ is a matrix (whose elements are built starting from two successive subsets taken on the training vector $\boldsymbol{x} \in \mathcal{X}$) and the kernel define in equation (3).

C. Abrupt change detection method

Let $(x_1, x_2, \ldots, x_t, \ldots, x_m)$ a set of observations defined in the space $\mathcal{X}$. The goal of the method is to detect whether or not there is an AC at the observation x_t. In that respect, two subsets corresponding to the immediate past $\boldsymbol{x}_1 = (x_{t-m_1}, \ldots, x_{t-1})$ and the immediate future $\boldsymbol{x}_2 = (x_t, \ldots, x_{m_2})$ of this observation are considered (Fig. 2 (b)). Two SV estimators based on a Gaussian kernel are separately trained from these subsets. The resulting parameters w_1, b_1 and w_2, b_2 will define the two separating hyperplanes $\mathcal{W}_1$ and $\mathcal{W}_2$.

Figure 2 (c) gives a geometrical representation of the KCD method whose main principle is to assess the possible occurrence of a rupture between the two subsets by comparing the arc $(c_{(t,1)}, c_{(t,2)})$ to the sum of the two arcs $(c_{(t,1)}, p_{(t,1)})$ and $(c_{(t,2)}, p_{(t,2)})$. Indeed, it computes a dissimilarity measure according to [12]:

$$D(x_1, x_2) = \frac{(c_{(t,1)}, c_{(t,2)})}{(c_{(t,1)}, p_{(t,1)}) + (c_{(t,2)}, p_{(t,2)})}, \quad (9)$$

where:

$$(c_{(t,1)}, c_{(t,2)}) = \arccos\left(\frac{\boldsymbol{\alpha}_1^t \boldsymbol{K}_{12} \boldsymbol{\alpha}_2}{\sqrt{\boldsymbol{\alpha}_1^t \boldsymbol{K}_{11} \boldsymbol{\alpha}_1} \sqrt{\boldsymbol{\alpha}_2^t \boldsymbol{K}_{22} \boldsymbol{\alpha}_2}} \right), \quad (10)$$

$$(c_{(t,j)}, c_{(t,j)})_{j=1,2} = \arccos\left(\frac{b_i}{\sqrt{\boldsymbol{\alpha}_j^t \boldsymbol{K}_{jj} \boldsymbol{\alpha}_j}} \right), \quad (11)$$

where α_1 (resp. α_2) is the column vector (Lagrange multipliers) corresponding to w_1 (resp. w_2) that have been computed during training. The kernel matrix $\boldsymbol{K}_{t,uv}, (u,v) \in \{1,2\} \times \{1,2\}$ has entries at row #j and column #l given $k(x_{t,u}^j, x_{t,v}^l)$, where $x_{t,u}^j$ is the observation #j in the subset x_u [8].

Finally, a decision index $I(t) = D(x_1; x_2)$ is compared to some predefined threshold η in order to decide whether a rupture occurred at position t.

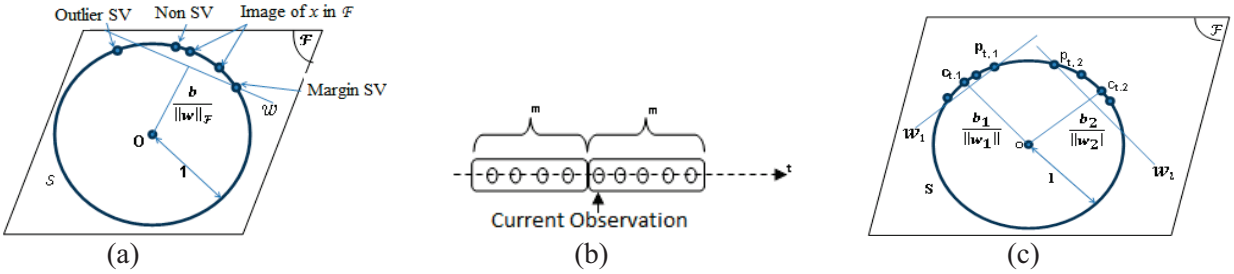

(a) (b) (c)

Fig. 2. (a) The SVM for the AC detection interpretation, (b) the scenario of the observations, and (c) geometrical representation of KCD method.

IV. APPLICATION OF THE KCD METHOD TO REAL EMI DATA

A. The aim of the proposed method

Figure 3 (a) shows the form of the induced voltage ΔV according to the EMI displacements for two real cases, where two cylindrical objects are buried at depth of 2 cm and 4,5 cm. As they are, the EMI system data does not provide much information about the object which is at the origin of this induced voltage. Particularly, in the case of the most buried object, the signature is almost invisible in the observation space. For this reason, we introduce KCD algorithm to make this information more meaningful. A decision index of

these previous EMI data is presented in Fig. 3 (b). In this case, one can see that the decision index of the most buried object is in the same magnitude of the second object.

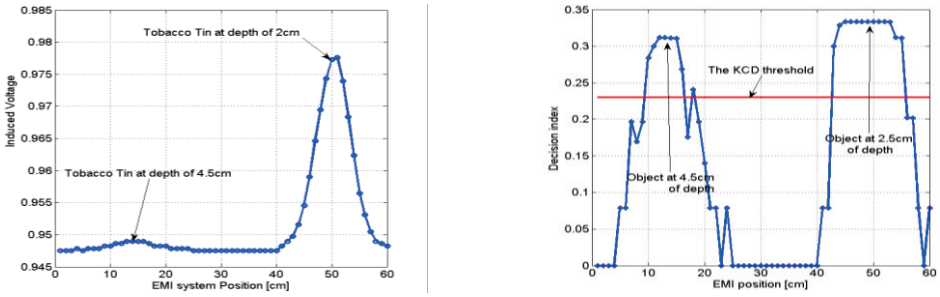

(a) (b)

Fig. 3. (a) Real EMI data (induced voltage ΔV) for two cylindrical objects buried at depth of 2 cm and 4,5 cm, and (b) decision index relative to these EMI data.

B. Overview of experimental tests performed

In this section, real cases of landmines detection are performed (a metal landmine and a plastic one), Fig. 4 (a). This testing was performed by the University of Florence-Italy in 2004, using multi-sensor system, in a bed with 3 m by 3 m in plan, with a sloping base at 60 cm to 80 cm to provide drainage, and minimize basal reflections. A multisensory system is used in the prospection. It includes the EMI system, GPR system and holographic radar system [16]. Four landmine simulants were buried at shallow depth in the test bed. These included:

- A PMA-2 simulant mine which reproduces the real PMA-2 anti-personnel plastic landmine with diameter of 6,9 cm. This landmine is buried at depth of 5 cm, Fig. 5 (a);
- Two cylindrical, metallic pipe tobacco tins with diameter of 10,5 cm. Those objects are buried at depths of 2 cm and 4,5 cm, Fig. 5 (b);
- A cylindrical plastic case with diameter of 10,5 cm. This object is buried at depth of 5,5 cm, Fig. 5 (c).

The objects were placed in the bed so as to form a square. The distance between the objects was 40 cm.

The exploration was made horizontally along parallel lines to sweep all the bed, Fig. 4 (b).

The EMI system provides a matrix of measurement points, which the number of rows is the number of the horizontal prospection lines and the number of columns is the number of the sampled measurement by line, Fig. 4 (b). In this case, all resulting responses of the EMI system give an image whose pixels are the points of measurements, and contrast of the pixel is the value of the induced voltage at these points.

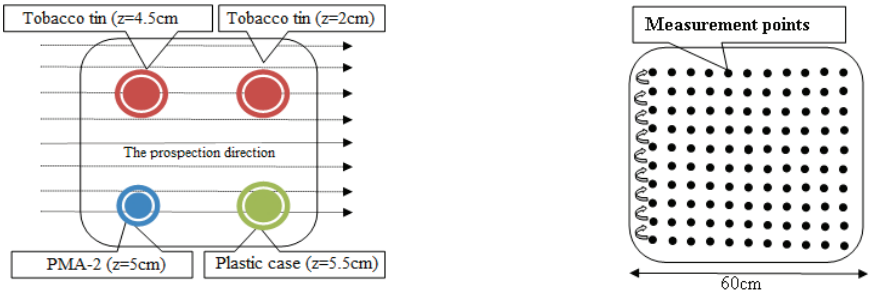

(a) (b)

Fig. 4. Schematic of buried landmine simulants: (a) objects position, and (b) prospection scenario; after a series of measurements with fixed step on the i^{th} horizontal line parallel to the X-axis, we shift for a fixed step following the Y-axis and we take again the same measurements on the $(i + 1)^{th}$ horizontal line.

C. Object detection using KCD algorithm

1) Parameters setting for EMI Data: the KCD method implementation requires several preliminary parameters settings:
   - The choice of the training subset larger m_1, m_2 : observations in a Bscan are made at a regular horizontally GPR displacement step. To ensure the rupture detection between two consecutive observations, the number of observations in the training subset multiplied by the GPR displacement step must be less than the half of the dimension of the object. Else, the KCD algorithm cannot detect a rupture since all the observations are in the same region of the observation space. Generally, we take $m_1 = m_2 = m$ where:
     $$m \times horizontal\_step \leq 0{,}5 \times object\_dimensions \quad (12)$$
   - Kernel Choice: The kernel defines implicitly the function $\phi_i : \mathcal{X} \to \mathcal{F}$. However, the elements presented below remain true for any Mercer kernel, such that satisfy the Mercer conditions defined in Section III-B [8], [9]. In the case of a Gaussian kernel, the σ sets the position of the sampled observations x_i in space $\mathcal{F}$. If $\sigma \ll \|x_i - x_j\|, (x_i, x_j) \in \mathcal{X}$, the dispersion of the observations images in $\mathcal{F}$ is important. Otherwise, all these images are close. Neither of these two cases is advantageous in the case of the rupture detection. A choice of σ approximately in the order of $\|x_i - x_j\|$ makes sense in this case [9], [11].
   - The choice of *v*: the parameter *v* determines the rate of inclusion of the abnormal observations. $v = 0$ corresponds to a hard margin algorithm. $v = 1$ corresponds to a margin released algorithm. In most cases, this parameter is taken between $0{,}2 \leq v \leq 0{,}8$.

   Generally, *v* and σ are selected in a heuristic way [11]. In our case, we used method IPSO described in [1] by taking some observations like entries for the optimization processes of these two parameters.

2) KCD algorithm for EMI Data: it is proposed to apply the KCD algorithm to detect the ruptures caused by the presence of the object using the EMI system in the previous measurements. To do this, the following steps are followed:

- Step 0: Initialization:
  – Generally the radius of the mines exceeds 3 cm. Since the horizontal step of displacement is 1 cm, we choose the size of the subsets $m_1 = m_2 = 3$.
  – The optimization process provided us the optimal $v = 0{,}5$ and $\sigma = 0{,}001$.
  – Set $t = m + 1$.
- Step 1: The Row Training:
  For each row of the resulting image, we do:
  – Initialized the subsets of training as $\boldsymbol{x}_1 = (x_{t-m}, \ldots, x_{t-1})$ and the immediate future $\boldsymbol{x}_2 = (x_t, \ldots, x_{t+m-1})$.
  – Trained independently the two subsets $\boldsymbol{x}_1$, $\boldsymbol{x}_2$ and we obtain the parameters $(w_{t,1}, b_1)$, $(w_{t,2}, b_2)$ or equivalently $(\alpha_{t,1}, b_1)$, $(\alpha_{t,2}, b_2)$.
  – Calculate the decision index $I_r(t) = D(\boldsymbol{x}_{t,1}, \boldsymbol{x}_{t,2})$ using (9-11).
- Step 2: The Increment:
  – If the maximum number of the points per row is reached, move to the next row.
  – Else increment $t \to t + 1$ and return to step 1.
- Step 3: The Columns Training:
  Once the scan of all rows is finished, we will have a decision index for each point of the image $I_r(t)$. Thereafter, we repeated the algorithm from step 1, but this time we consider the columns for the construction of the subsets. The test of step 2 is compared to the number of points per column for the passage to the next column. A decision index I_c is also calculated for each point and the global decision index for each point will be the sum of the two decision indexes.
  $$I_t = I_r + I_c. \quad (13)$$
- Step 4: On Line Rupture Detection:
  Once the total decision index is computed, the resulting image is tainted with some

residues, due to the roughness of the soil. However, the decision index magnitude of these residues is low compared to that of the objects, and to eliminate them, a thresholding is applied to the image to make it clearer, and the rupture detection is tested using:

– If $I_t(t) \geq \eta$ there is a rupture in instant t.

– If $I_t(t) < \eta$ there is no rupture in instant t.

D. The choice of rupture threshold η:

Figure 3 (a) shows the response of the EMI system for the horizontal line which passes over the two Tobacco tin objects. Note that, for the most buried object, the response is almost zero. In this case, the detection is difficult by working directly on the data in the observation space. Figure 3 (b) shows the decision index response of the EMI using the KCD algorithm applied to the EMI response of the Fig. 3 (a). Note that in this case, the response of the more buried object is more visible and which is exactly the interest of the proposed method. A threshold of $\eta = 0,23$ is acceptable in this case. Thus, for the values lower than the threshold, the background noise of the image will be considered as null. In this case, the image will be clear and the problem of noise will be solved.

E. Results and discussion

Figure 6 (a) shows the EMI response on the studied bed. It is revealed that, for the most buried object, the response is almost not visible. Indeed, the detection of this object is not evident in the observation space.

The introduction of KCD algorithm for the rupture detection based on SV-estimators becomes a necessity. Therefore, whatever the depth of the object, the algorithm KCD must detect the ruptures in the EMI response. Figure 6 (b) shows the decision index of the EMI response system without thresholding. Although, we can distinguish objects but the resulting image is tainted yet.

After a good thresholding, we have Fig. 6 (c), where all metal objects are clearly visible. We note that, the two tobacco tins are located with their precise positions and the distance between the two metal objects is 40 cm. Then, if the object is largely buried, the method provides information on the dimensions of the object even if the signature of the object is low. In this case, the diameter of the two objects is 10 cm.

The total time for processing data (3600 samples of the induced voltage corresponding to a surface scan of 60 cm × 60 cm with a step of 1 cm, Fig. 4 (b)) is $148,24s$. For the KCD treatment of one sampled induced voltage we need $41,17ms$, which makes the real-time detection possible.

Unfortunately, since the EMI system only detects the metallic objects, the other two plastic objects are not visible because of the absence of their signatures.

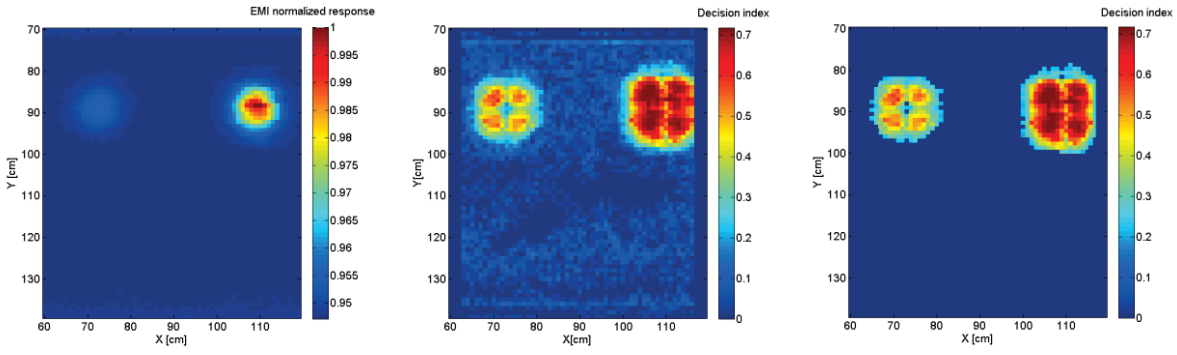

Fig. 6. (a) EMI response, (b) the total decision index without thresholding, and (c) the total decision index with thresholding.

V. CONCLUSION

The proposed method is based on the KCD algorithm and SV-training. A decision index is calculated from measurements provided in the case of an EMI inspection in a hypotheses space according to both horizontal and vertical axes. We have noticed that, for different depths of buried objects, the decision index magnitude is almost the same. Then, we set a threshold to remove more residues that are due to the roughness of the ground. An image of the soil basement is generated highlighting different objects located therein. The method was tested on real EMI data made available by the University of Florence, Italy. This test has given good results for the detection and identification of buried metallic objects.

ACKNOWLEDGMENT

The authors would like to thank Timothy D. Bechtel, Ph.D., PG Visiting Professor, Department of Earth and Environment Franklin and Marshall College, Lancaster, PA, USA for his contribution in this work and the real GPR data that provided us.

REFERENCES

[1] Y. Matriche, M. Feliachi, A. Zaoui, and M. Abdellah, "An EMI inversing problem for landmine characterization based on improved particle swarm optimization and finite element analysis," *Progress In Electromagnetics Research, B*, vol. 49, pp. 411-428, March 2013.

[2] K. Paulsen, I. Shamatava, F. Shubitidze, K. O'Neill, and K. Sun, "Fundamental mode approach to forward problem solutions in EMI scattering inferring fundamental solutions from training data," *Applied Computational Electromagnetics Society-Conference Computational Techniques*, 2004.

[3] K. P. Prokopidis and T. D. Tsiboukis, "Modeling of ground-penetrating radar for detecting buried objects in dispersive soils," *Applied Computational Electromagnetics Society*, vol. 22, no. 2, 2007.

[4] H. Huang, B. SanFilipo, A. Oren, and I. J. Won, "Coaxial coil towed EMI sensor array for uxo detection and characterization," *Journal of Applied Geophysics*., vol. 61, no. 3-4, pp. 217-226, March 2007.

[5] F. Shubitidze, J. P. Fernandez, I. Shamatava, L. R. Pasion, B. E. Barrowes, and K. O'Neill, "Application of the normalized surface magnetic source model to a blind unexploded ordnance discrimination test," *Applied Computational Electromagnetics Society*, vol. 25, no. 1, 2010.

[6] S. Saidi and J. B. S. Hadj, "Improving convergence time of the electromagnetic inverse method based on genetic algorithm using the PZMI and neural network," *Progress In Electromagnetics Research, B*, vol. 51, pp. 389-406, April 2013.

[7] M. Mahmoudi and S. Y. Tan, "Depth detection of conducting marine mines via eddy-current and current-channeling response," *Progress In Electromagnetics Research, PIER*, vol. 90, pp. 287-307, 2009.

[8] F. Desobry and M. Davy, "Support vector-based online detection of abrupt changes," *Proceedings IEEE Int. Conf. Acoust. Speech, Signal Process, (ICASSP 03)*, vol. 4, pp. 872-875, 2003.

[9] F. Desobry, M. Davy, and C. Doncarli, "An online kernel change detection algorithm," *IEEE Trans. Signal Process*, vol. 53, no. 8, pp. 2961-2974, August 2005.

[10] M. Al Sharkawy, M. Sharkas, and D. Ragab, "Breast cancer detection using support vector machine technique applied on extracted electromagnetic waves," *Applied Computational Electromagnetics Society*, vol. 27, no. 4, 2012.

[11] D. Potin, P. Vanheeghe, E. Duflos, and M. Davy, "An abrupt change detection algorithm for buried landmines localization," *IEEE Trans. Geosci. Remote Sensing*, vol. 44, no. 2, pp. 260-272, 2006.

[12] S. Caorsi, D. Anguita, E. Bermani, A. Boni, and M. Donelli, "A comparative study of NN and SVM-based electromagnetic inverse scattering approaches to on-line detection of buried objects," *Applied Computational Electromagnetics Society*, vol. 18, no. 2, 2003.

[13] V. Vapnik, "The nature of statistical learning theory," 2nd ed., *Ser. Statistics for Engineering and Information Science, Springer*, 1999.

[14] T. Coleman and Y. Li, "A reflective Newton method for minimizing a quadratic function subject to bounds on some of the variables," *SIAM Journal on Optimization*, vol. 6, no. 4, pp. 1040-1058, 1996.

[15] N. Gould and P. L. Toint, "Preprocessing for quadratic programming," *Mathematical Programming, Series B*, vol. 100, pp. 95-132, 2004.

[16] L. Capineri, S. Ivashov, T. Bechtel, A. Zhuravlev, P. Falorni, C. Windsor, G. Borgioli, I. Vasiliev, and A. Sheyko, "Comparison of GPR sensor types for landmine detection and classification," *12th International Conference on Ground Penetrating Radar*, 2008.